Molecular Vision 2014; 20:593-605 <http://www.molvis.org/molvis/v20/593>
Received 7 June 2013 | Accepted 30 April 2014 | Published 2 May 2014

© 2014 Molecular Vision

Downregulation of β-actin and its regulatory gene *HuR* affect cell migration of human corneal fibroblasts

R. Joseph,[1] O.P. Srivastava,[1] R.R. Pfister[2]

[1]Department of Vision Sciences, University of Alabama at Birmingham, Birmingham, AL; [2]Eye Research Laboratory, Eye Research Foundation, Birmingham, AL

Purpose: In an earlier study, we showed that human antigen R (HuR) and β-actin expression levels were downregulated in fibroblasts isolated from human keratoconus stroma compared to normal corneal stroma. To further extend the finding, we determined whether HuR expression affects β-actin gene expression and in turn affects corneal fibroblast migration and wound healing.

Methods: Stromal keratocytes from normal human corneas were cultured in the presence of serum. Cells were transfected with siRNA specific for β-actin or HuR. SiRNAs specific for GAPDH or a scrambled sequence were used as positive and negative controls (siCTR) for transfection, respectively. The effects of gene silencing were analyzed at the transcriptional and translational levels. Specific proteins were immunohistochemically localized using confocal imaging. The effects of gene silencing on cell migration and cell proliferation were analyzed using a modified Boyden chamber and with a wound healing assay, respectively.

Results: Reverse-transcription PCR (RT–PCR) and western blot analyses showed that when the *HuR* gene was silenced, β-actin expression was significantly downregulated. This was further confirmed at the translational level with immunohistochemical-confocal analysis. However, when the *β-actin* gene was silenced, its expression was significantly decreased but showed no effect on *HuR* gene expression. When the *β-actin* or *HuR* gene was individually silenced, the motility and proliferation of corneal fibroblasts were significantly reduced.

Conclusions: The results show that downregulation of the *HuR* gene results in decreased β-actin gene expression, which in turn results in decreased motility and proliferation of corneal fibroblasts. We conclude that decreased β-actin expression in normal corneal stroma clearly disrupts the cytoskeletal structure and functions, including keratocyte motility and wound healing.

The functional attributes of any cell are mainly regulated by cytoskeletal integrity and signaling, with actins playing a role as one of the major cytoskeletal structural proteins of eukaryotic cells. Actins are involved in many cellular processes, including cell adhesion, cell migration/movement, cytokinesis, endo-/exocytosis, cell division, signal transduction, mRNA localization, and transcription. Eukaryotes have six actin isoforms; each is encoded by an individual gene [1]. Among the six actin isoforms, two are striated muscle-associated (α-skeletal and α-cardiac muscle actins), two smooth muscle-associated (α- and γ-smooth muscle actins), and two are cytoplasmic (β-and γ-actins) [2]. The muscle actins are tissue-specific and constitute the contractile units, whereas β- and γ-actins are ubiquitous, and are essential for cell survival [3]. The actin isoforms have highly conserved amino acid sequences. They differ mainly at their N-termini, whereas the cytoplasmic β- and γ-actins differ by only four amino acids. The absence of β-actin at the embryonic stage was lethal in a transgenic mouse model [4]. β-actin exists as a globular (G-actin) or filamentous actin (F-actin); the latter is arranged in the form of strings of uniformly oriented G-actin subunits in a tight helix.

The normal expression levels of β-actin mRNA are important for these cellular processes. The expression of the *actin* gene (ACTB, OMIM 102630) is regulated at the transcriptional [5] and post-transcriptional levels, each at the cellular localization of their mRNAs [6]. The embryonic lethal abnormal vision (ELAV) family of proteins, in particular the HuC (mouse) and human antigen R (HuR), have been shown to exhibit poly(A)–binding activity, and simultaneously bind to the AU-rich elements (ARE) and the poly(A) tail in vitro [7,8]. The mRNA of HuR is ubiquitously expressed in all proliferating cells, and is the most important post-transcriptional regulator of gene expression [9]. Dormoy-Raclet et al. have shown that HuR depletion in HeLa cells alters the cytoskeleton functions influencing cell adhesion, migration, and invasion [10]; all are attributable to the loss of β-actin stress fibers. HuR binding to the U-rich element is involved in β-actin mRNA stability, and the binding stabilizes the half-life of β-actin mRNA [5,11].

Correspondence to: O.P. Srivastava, Department of Vision Sciences, 924 18th Street South, University of Alabama at Birmingham, Birmingham, AL 35294-4390; Phone: (205) 975-7630; FAX: (205) 934-5725; email: srivasta@uab.edu

Our previous studies on keratoconus stroma showed that β-actin and HuR expression levels were downregulated at the mRNA and protein expression levels compared to normal stroma. This raised the possibility that downregulation of HuR and β-actin could be a result of the interplay between the two [12]. In the present study, we used siRNA-mediated gene knockdown to determine if *HuR* gene silencing affects the stability of β-actin mRNA. The decreased HuR expression resulted in decreased β-actin gene and protein expression leading to decreased fibroblast wound healing and their proliferation.

METHODS

Human corneas: Normal corneas, stored in Optisol (Chiron Ophthalmics, Irvine, CA) at 4 °C, were obtained within 12 h after enucleation from the Alabama Eye Bank. The central 8-mm region of the normal corneas was trephined and recovered. The epithelium and the endothelium were scraped off, leaving the stroma to be used in these experiments. The procurement of human corneas in this study was approved by the Institutional Review Board of the University of Alabama at Birmingham, following the tenets of the Declaration of Helsinki for Research Involving Human Subjects.

Cell culture and transfection: The stroma was incubated overnight in collagenase (1 mg/ml; Worthington, Lakewood, NJ). The resulting keratocytes were washed in Dulbecco's modified Eagles medium (DMEM; Invitrogen, Grand Island, NY) containing 1% antibiotics (penicillin-streptomycin solution, Mediatech, Herndon, VA). The primary cultures of human corneal fibroblasts were established [12], and the cells from passage 2 were used for this study. The cells were then seeded onto six-well plates (Corning, Franklin Lakes, NJ) in DMEM containing 10% fetal bovine serum (Hyclone, Logan, UT) and 1% antibiotics (penicillin-streptomycin solution) at 37 °C in a 5% CO_2. Four individual cell cultures were generated from four different donor corneas, and all experiments were performed using these cultures.

Gene knockdown studies: Knockdown of HuR or β-actin genes in normal human corneal fibroblasts was performed using siRNA duplexes. The siRNA transfection was done on fibroblasts derived from four different corneas. The cells were plated at 1.5×10^5 cells per well in a six-well plate and grown overnight at 37 °C with 5% CO_2. The silencer select, predesigned, and validated siRNA sequences were purchased from Ambion (Life Technologies, Invitrogen, Cambridge, MA). The siRNA sequences that targeted the specific coding regions of GAPDH (used as a positive control), β-actin, or HuR were used. In addition, a nonspecific, scrambled siRNA duplex was used as a control to examine its effect of transfection, and it was denoted as siCTR. A dose-response curve established that the 5 nM concentration of siRNA gave an optimal response in transfected cells. We used a scrambled sequence and the GAPDH siRNA as the siRNA controls. The siRNA sequences were diluted in OPTI-MEM1 reduced medium (Invitrogen, Grand Island, NY) and transfected using Lipofectamine Plus (Invitrogen, Carlsbad, CA) using the manufacturer's protocol. The cells were processed at 24 h and 72 h after transfection to determine the expression of the targeted genes at the transcriptional and translational levels. The following siRNA duplex sequences were used: HuR (5′-GCG UUU AUC CGG UUU GAC ATT UGU CAA ACC GGA UAA ACG CAA-3′; β-actin (5′-CCU GUA CAC UGA CUU GAG ATT UCU CAA GUC AGU GUA CAG GTA-3′). Proteins were recovered from cultured corneal fibroblasts after transfection and homogenization in radioimmunoprecipitation assay (RIPA) buffer (Thermo Scientific, Rockford, IL).

Reverse transcription–PCR and real-time PCR analysis: The reverse transcription–PCR (RT–PCR) analysis was performed using the Access RT–PCR system (Promega, Madison, WI), with 500 ng of RNA. The primers were designed using Primer 3 for β-actin, HuR, and GAPDH are as follows: β-actin forward (5′-GTT GCT ATC CAG GCT GTG-3′); β-actin reverse (5′-TGA TCT TGA TCT TCA TTG TG-3′); HuR forward (5′-ATG AAG ACC ACA TGG CCG AAG ACT-3′); HuR reverse (5′-AGT TCA CAA AGC CAT AGC CCA AGC-3′); GAPDH forward (5′-GAG TCA ACG GAT TTG GTC GT-3′); GAPDH reverse (5′-TTG ATT TTG GAG GGA TCT CG-3′). The PCR products were analyzed using agarose gel electrophoresis. Images were captured with a gel documentation system. Four fibroblast cultures from four different normal corneas were used for gene silencing, and experiments were performed in triplicate. Real-time PCR quantification was performed using the Bio-Rad iCycler iQ system (Bio-Rad, Hercules, CA). Real-time quantitative PCR (qPCR) was performed using 96-well reaction plates in a total volume of 25 µl. The reaction mixture included 12.5 µl of Real-Time SYBR Green PCR Master Mix (Bio-Rad), 2.5 µl of reverse transcription product, 1 µl of forward and reverse primers, and 8 µl of DNase/RNase free water. The reaction mixtures were initially heated at 95 °C for 10 min to activate the polymerase, followed by 40 cycles, which consisted of the denaturation step at 95 °C for 15 s, annealing at 56 °C for 60 s, and the elongation step at 72 °C. The data were normalized to 18S RNA. The qRT-PCR data were analyzed with the comparative ΔCt method.

Western blot analysis: Samples containing 30 µg protein were lysed with 1X sodium dodecyl sulfate (SDS) gel-loading

buffer and analyzed with SDS–polyacrylamide gel electrophoresis (SDS–PAGE) using 12% polyacrylamide gels [13]. Proteins were transferred to a polyvinylidene fluoride membrane (Bio-Rad) by using a semidry transfer cell (Bio-Rad, Trans-blot SD), and blocked with 3% nonfat milk in PBS (1X; 137 mM NaCl, 2.7 mM KCl, 10 mM Na_2HPO_4, 2 mM KH_2PO_4, pH 7.4) for 1 h at room temperature. The membranes were probed with anti-β-actin monoclonal antibody (Sigma, St. Louis, MO) at a 1:100 dilution, followed by incubation in goat anti-mouse secondary antibody conjugated to infrared fluorescent dye (IRD; LI-COR Biosciences, Lincoln, NE) at 1:10,000 dilution. Blots were scanned using the Odyssey Imaging system (LI-COR Biosciences). If reprobing of a blot was desired, the antigen-antibody complex was stripped using a mild stripping solution (0.2 M glycine-HCl, pH 2.2, 0.1% SDS, 0.01% Tween-20) for 1 h at room temperature, followed by 3X washing with PBS-0.1% Tween-20. The membranes were then blocked as described and reprobed with anti-vimentin monoclonal antibody (Sigma) at 1:200 dilution, followed by incubation with the secondary antibody as described, and scanning using the Odyssey Imaging system. The pixel intensity of the western blots, normalized to vimentin, was analyzed using Image-J software [14]. The normalized value of siCTR was considered 100%, and the other values were calculated compared to the siCTR value. The results are shown in a bar graph with standard deviations.

Immunofluorescence-confocal Imaging: Normal corneal fibroblasts were seeded on 18-mm cover-glasses for 24 h, and then the cells were transfected as described in the Methods section. After 72 h, the cells were fixed with 4% formaldehyde for 30 min at room temperature, and washed three times with PBS. The cells were permeabilized by incubation in 0.5% Triton X-100 in PBS for 10 min, followed by washing three times in PBS. The cells were then incubated with a blocking solution containing 10% normal serum and 0.5% bovine serum albumin (BSA) in PBS for 1 h, and incubated with the desired primary antibody at 4 °C for 24 h. Next, the cells were washed three times in PBS, followed by incubation with a secondary antibody for 1 h in the dark. The cells were washed three times in PBS, and incubated with Hoechst nuclear stain for 10 min, washed again one time in PBS, and mounted on slides with a mounting medium (Fluromount-G, Southern Biotech, Birmingham, AL). Mouse immunoglobulin G (IgG) was used as a negative control with the identical protein concentration as that of the primary antibodies. Confocal imaging was performed using a Zeiss LSM 710 confocal microscope (Carl Zeiss Microscopy, Göttingen, Germany) at the High Resolution Imaging Facility of the University of Alabama at Birmingham.

Cell migration assay: A modified Boyden chamber was used for the cell migration assay. We used a 96-well format ChemoTx system (Neuro Probe, Gaithersburg, MD), and the experiment was performed according to the manufacturer's protocol. The siRNA transfection was performed with four different human corneal fibroblast cells. Forty-eight hours after transfection with the siRNA duplexes, the corneal fibroblasts were trypsinized, resuspended in serum-free medium, and seeded in the upper chamber of the Boyden chamber. The reservoir of the chamber was filled with complete medium containing 10% fetal bovine serum (FBS), and cells were allowed to migrate to the lower surface through a filter for 22 h at 37 °C. The cells that remained in the top membrane surface were thoroughly wiped out using a moistened Kimwipe (Kimberly-Clark Global Sales, Roswell, GA). Next, the membrane was cut out and inverted on a slide. The cells that had migrated to the lower surface were stained using hematoxylin stain. The siRNA treatment and the cell migration assay were performed in triplicate. The migratory cell images were photographed using the Zeiss AxionPlan 2 Imaging System Microscope (Carl Zeiss Microscopy, Thornwood, NY) at the Core Facility of Vision Sciences Research Center of the University of Alabama at Birmingham. The cells were counted from six images, and the data are presented with standard deviations.

Wound healing assay: The cells were plated at 1.5×10^5 cells per well of a 12-well plate and grown overnight at 37 °C with 5% CO_2. The siRNA transfection was performed on four different human corneal fibroblast cells. The 80% confluent cells were treated with siRNA as described, and after 72 h, a straight line scratch was made on a confluent monolayer of cells using a sterile 1 ml disposable serological pipette. To remove debris and smooth the edge of the scratch, the cells were washed with 1 ml DMEM. Images of the cell proliferation were taken using a Nikon Eclipse TS100 microscope (NiKon Eclipse TS 100 , Southern Micro Instruments, Marietta GA) at 0 h and 24 h after the scratch with a Nikon Coolpix camera attached to the microscope. The siRNA treatment and the scratch assay were performed in triplicate. The cells were counted manually at 0 h and after 24 h post-scratch from six images, and the data are presented with standard deviations. To observe the effects of phosphatidylinositol 3-kinase (PI3K) inhibition, the cells were treated with 10 µM LY 292,004 (Sigma) for 24 h after wounding. A p value of <0.05 was judged (±standard error of the mean [SEM]) to be statistically significant as determined by the Student *t* test.

RESULTS

Human antigen R knockdown leads to a decrease in β-actin expression in stromal fibroblasts at transcriptional and translational levels: Our previous results showed downregulation in the expression of *β-actin* and *HuR* genes in keratoconus corneal stroma relative to normal corneas [12]. In the present study, we used RNAi-mediated gene silencing for β-actin or HuR in normal corneal fibroblasts to understand the respective gene functions. The *GAPDH* gene and scrambled sequence (which do not affect any targeted genes) were used as positive and negative controls for transfection, respectively. The sequences of the siRNA duplex were selected from the coding region of the desired target mRNAs, and the transfection was performed as described in the Methods section. The desired mRNA levels were analyzed using RT–PCR at 24 h post-transfection. Figure 1A(I) shows *β-actin* gene expression using β-actin primers after transfection of human corneal fibroblasts with the scrambled siRNA, siGAPDH, siβ-actin, or siHuR. Expression of the *β-actin* gene was downregulated after the *HuR* gene was silenced, which suggested that HuR has a regulatory role in *β-actin* gene expression. Additionally, *β-actin* gene silencing also showed downregulation of the *β-actin* gene, which was used as the control. Figure 1A(II) shows *HuR* gene expression using HuR primers after transfection of human corneal fibroblasts with siRNA for scrambled, GAPDH, β-actin, or HuR. Expression of the *HuR* gene was downregulated on *HuR* gene silencing, whereas *β-actin* gene silencing had no effect on HuR expression. Figure 1B shows western blot analysis of β-actin expression after transfection with the siRNA of scrambled, GAPDH, β-actin, and HuR. The western blot results show the reduced expression of β-actin and HuR relative to vimentin (used as the control). For visualization of vimentin with anti-vimentin antibody, the blot that was used for β-actin visualization was stripped and used again for the vimentin visualization. RT–PCR analysis showed that after 24 h, *GAPDH* gene silencing had no effect, and the expression remained at the same level (data not shown), which was confirmed with the western blot analysis. Figure 1C shows the percentage of β-actin expression levels after they normalized to vimentin and calculated as described in the Methods section. Relative to the expression of vimentin, the levels of β-actin expression were 24% and 18% lower after *HuR* and *β-actin* gene silencing, respectively. This suggests that the loss of HuR results in downregulation of the *β-actin* gene. There was no change in the β-actin expression levels after the *GAPDH* gene or negative control (siCTR) was silenced. Figure 1D shows the real-time PCR analysis after 72 h of siRNA treatments for the *siCTR*, *GAPDH*, *HuR*, and *β-actin* genes. The y-axis in the figure shows the relative fold expression, and the x-axis shows the β-actin primer used for the real-time PCR analysis. *β-actin* gene expression decreased by 80–90% after the *β-actin* and *HuR* genes were silenced, which was similar to the RT–PCR analysis. Whereas *GAPDH* gene silencing suppressed *β-actin* gene expression after 72 h of gene silencing (Figure 1D).

Localization of proteins after downregulation of their genes using immunohistochemical-confocal imaging: To further verify the western blot results, we used confocal imaging to localize the individual proteins after siRNA treatment. We analyzed whether β-actin gene silencing affected HuR expression in corneal fibroblasts (Figure 2). Figure 2 shows the immunoreactivity to the anti-HuR antibody of the corneal fibroblasts transfected with GAPDH siRNA, HuR siRNA, or β-actin siRNA. The effect on *HuR* gene expression was analyzed after the *GAPDH* gene was silenced. Figure 2A,D,G show Hoechst nuclear staining (blue fluorescent staining), and Figure 2B,E,H shows the immunoreactivity to the anti-HuR antibody. Green fluorescent staining in the nuclear region (punctate in appearance) was observed on immunoreactivity with the anti-HuR antibody in the cells treated with siGAPDH (Figure 2B), and with β-actin siRNA (Figure 2E). Figure 2C,F,I is an overlay of Figure 2A,B,D,E,G,H. *GAPDH* gene silencing had no effect on *HuR* gene expression. *β-actin* gene silencing had no effect on the expression of HuR as represented by the presence of green fluorescent staining in the nuclear region (Figure 2E). The effect of *β-actin* gene silencing on HuR expression was in concordance with our previously described RT–PCR and western blot results. In contrast, *HuR* gene silencing resulted in the loss of *HuR* expression, which representing a loss of green punctate fluorescent staining (Figure 2H). Together, the results show that HuR expression was downregulated in corneal fibroblasts after transfection with HuR siRNA (Figure 2H), whereas *β-actin* and *GAPDH* gene silencing had no effect on HuR expression (Figure 2B,E).

Next, we analyzed whether *HuR* gene silencing affects *β-actin* gene expression (Figure 3). Figure 3 shows the immunoreactivity of corneal fibroblasts to the anti-β-actin antibody following transfection with GAPDH siRNA, HuR siRNA, or β-actin siRNA. F-actin was visualized by using rhodamine-labeled phalloidin (toxin from the mushroom *Amanita phalloides*). Figure 3A,E,I,M shows the Hoechst nuclear blue stain, and Figure 3B,F,J,N shows the immunoreactivity to the anti-β-actin antibody of the corneal fibroblasts after transfection with scrambled siRNA, siGAPDH, siHuR, or siβ-actin, respectively. The scrambled siRNA treatment showed no effect on β-actin expression as seen by the presence of uniform green fluorescent stain in cells with the anti-β-actin antibody (Figure 3B). Figure 3C,G,K,O shows

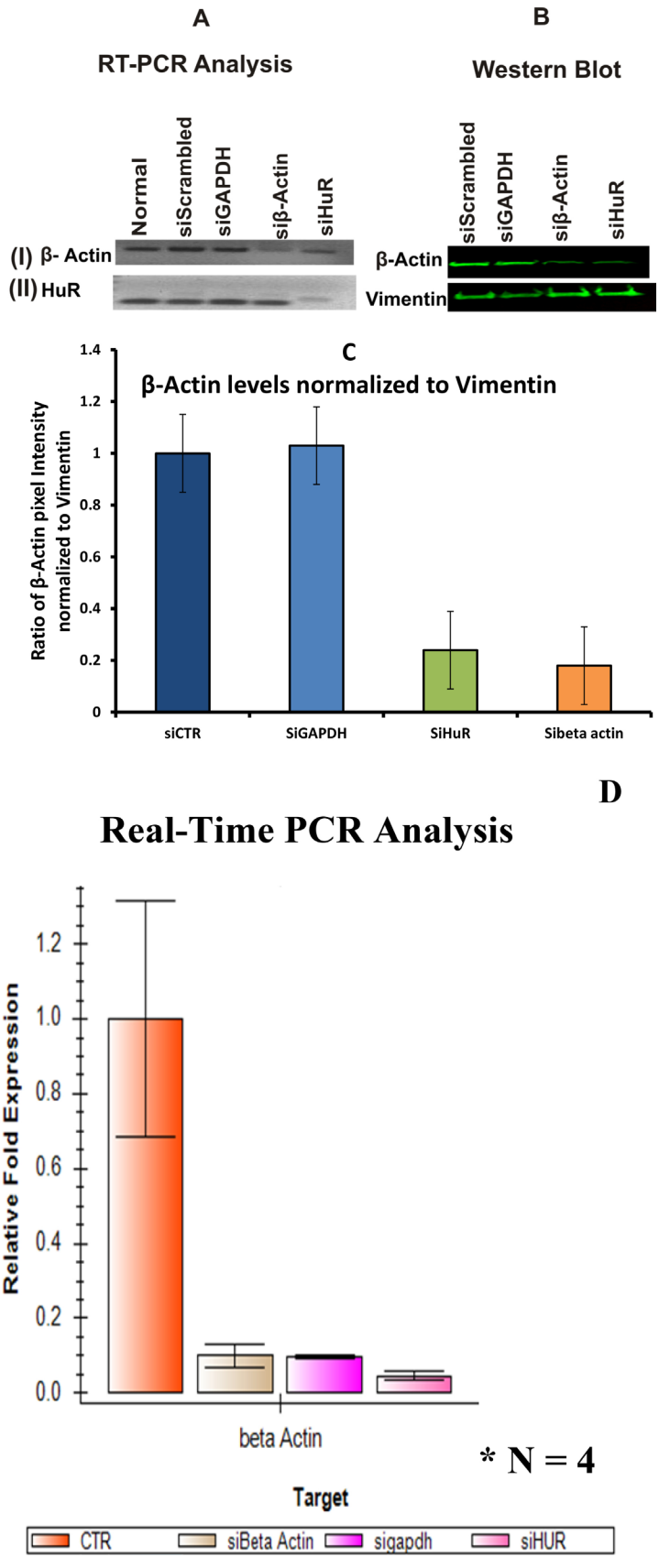

Figure 1. Gene expression analysis after gene silencing. **A**: Detection of the expression of glyceraldehyde 3-phosphate dehydrogenase (*GAPDH*), *β-actin*, and human antigen R (*HuR*) genes after gene silencing using RT–PCR. In the analyses, cells were examined 24 h after the treatments. In (**A**), (I): RT–PCR analysis of β-actin gene expression in corneal fibroblasts after gene silencing using siScrambled, siGAPDH, siβ-actin, or small interfering human antigen R (siHuR). (II): RT–PCR analysis of *HuR* gene expression in corneal fibroblasts after gene silencing using siScrambled, siGAPDH, siβ-actin, or siHuR. **B**: Western blot analysis of β-actin expression using the anti-β-actin antibody in corneal fibroblasts after gene silencing using siScrambled, siGAPDH, siβ-actin or siHuR. Vimentin expression was used as a control. β-Actin expression was downregulated on either *β-actin* gene silencing or that of *HuR* gene. **C**: A bar graph shows the percent of β-actin levels after the gene silencing. **D**: Real-time PCR analysis of the *β-actin* gene after the following treatments: siScrambled (siCTR), siGAPDH, siβ-actin, and siHuR.

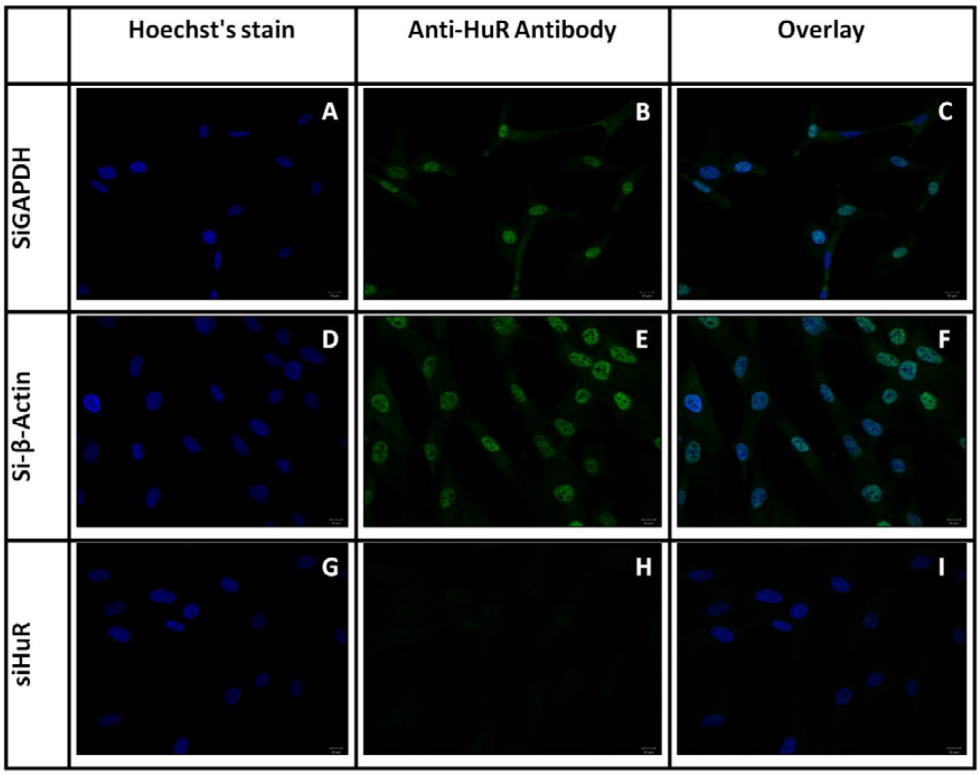

Figure 2. Localization of human antigen R after gene silencing. The normal corneal fibroblasts were treated with GAPDH siRNA, β-actin siRNA, or human antigen R (HuR) siRNA. The immunoreactivity of HuR was analyzed at 72 h post-transfection. **A**: Fibroblasts stained with Hoechst nuclear stain after a treatment with GAPDH siRNA. **B**: Immunoreactivity of fibroblasts with anti-HuR antibody after a treatment with GAPDH siRNA. **C**: Overlay of (**A**) and (**B**). **D**: Fibroblasts stained with Hoechst nuclear stain after a treatment with β-actin siRNA. **E**: Immunoreactivity of fibroblasts with anti-HuR antibody after a treatment with β-actin siRNA. **F**: Overlay of (**D**) and (**E**). **G**: Fibroblasts stained with Hoechst nuclear stain after treatment with HuR siRNA. **B**: Immunoreactivity of fibroblasts with anti-HuR antibody after treatment with HuR siRNA. **C**: Overlay of (**G**) and (**H**). Note that the GAPDH siRNA and β-actin siRNA treatments had no effect on HuR expression and its nuclear localization. *HuR* gene silencing significantly reduced the expression of HuR, as shown by the absence of green fluorescence in nuclei.

F-actin staining with rhodamine-labeled phalloidin (red fluorescence), following transfection with scrambled siRNA, siGAPDH, siHuR, or siβ-actin, respectively. Figure 3D,H,L,P shows an overlay of Hoechst nuclear stain, immune-stain with anti-β-actin antibody, and F-actin staining after transfection. Together, the results show that scrambled siRNA treatment had no effect on *β-actin* gene expression.

On examination of the effects of GAPDH knockdown on β-actin expression (Figure 3E–H), decreased levels of green fluorescence (due to β-actin [Figure 3F]) and red fluorescence (due to F-actin [Figure 3G]) were observed. Together, the results showed that β-actin expression affected *GAPDH* gene silencing (Figures 3F,G), whereas it remained unaffected with the use of scrambled siRNA. We analyzed the effect of *HuR* gene silencing on *β-actin* gene expression (Figure 3I–K), which showed an absence of green fluorescence (due to β-actin, Figure 3J) and decreased red fluorescence (staining F-actin; Figure 3K). β-actin gene knockdown was used as a positive control to examine the effects of gene silencing. Similarly, *β-actin* gene knockdown (Figure 3M–P) resulted in an absence of green fluorescence (due to β-actin, Figure 3N) and decreased red fluorescence of F-actin (staining F-actin, Figure 3O). Together, the results suggested that the silencing of *HuR* or *β-actin* gene (Figure 3J,N) resulted in downregulation of the *β-actin* gene, as observed earlier during western blot analysis (Figure 1B). Further, the *HuR* gene seems to be a stability factor for β-actin mRNA, and plays a role in gene expression. In contrast, the *β-actin* gene had no effect on *HuR* gene expression. However, the downregulation of the *β-actin* gene after gene silencing of GAPDH (Figure 3F) was a surprise to us, and has been shown for the first time.

Effects of gene silencing on migration of normal corneal fibroblasts: Next we analyzed the functional significance of the loss of the *HuR* gene and whether it leads to a loss in the cytoskeletal function such as corneal fibroblast migration. Cell migration is an important biologic process mainly generated by the β-actin cytoskeleton [3]. The modified Boyden chamber assay was used to determine if targeted deletion of the *HuR* or *β-actin* gene affected migration of normal corneal fibroblasts. Figure 4A shows the migrated cells (pointed arrows denote the cells) in the corneal fibroblasts, and Figure 4B,C,D,E shows cell migration following silencing of scrambled siRNA, and siRNA of the *GAPDH* gene, *HuR* gene, or *β-actin* gene, respectively. Cells migrated per image (Figure

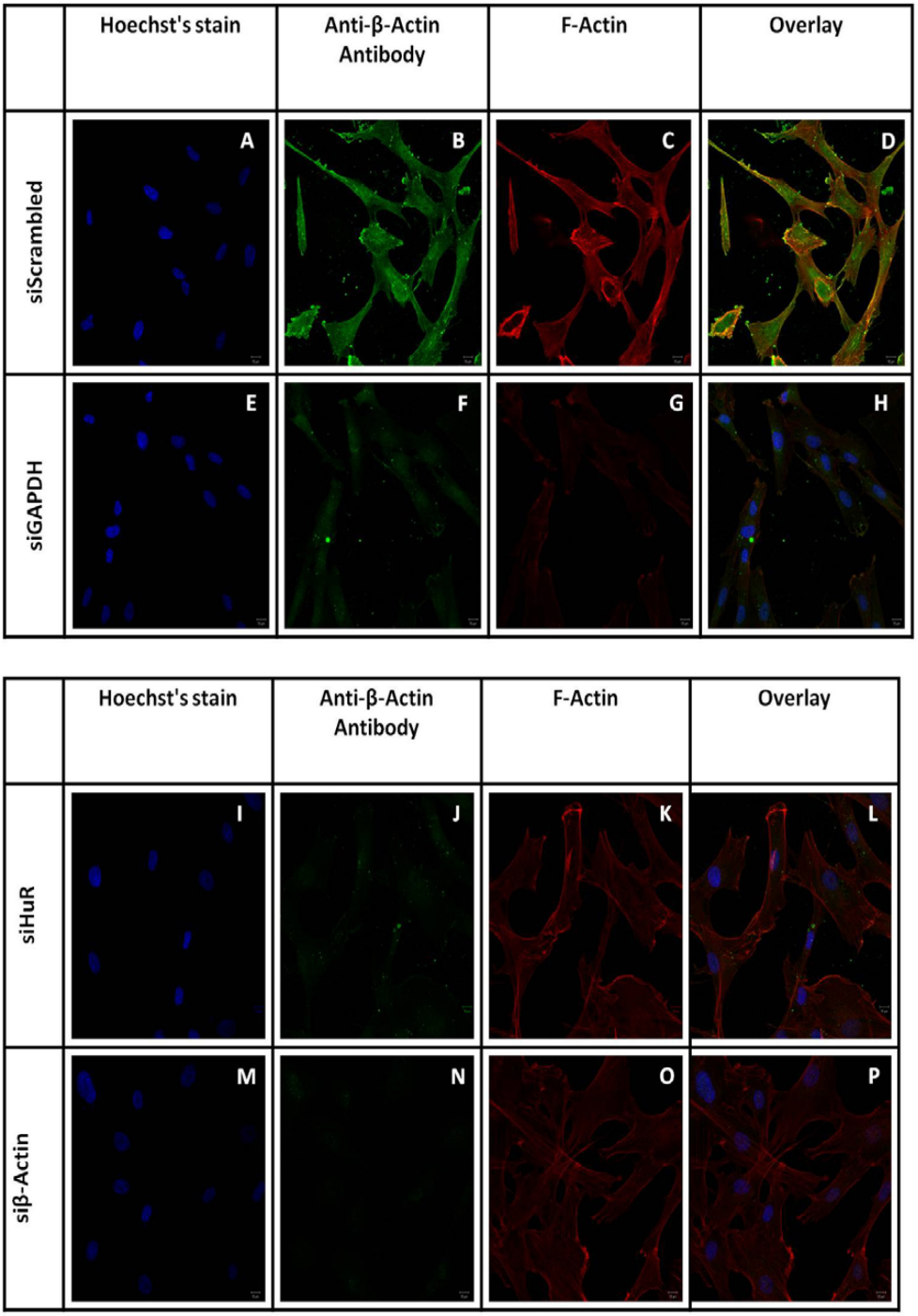

Figure 3. Localization of β-actin in corneal fibroblasts after gene silencing. The normal corneal fibroblasts were treated with scrambled siRNA, GAPDH siRNA, β-actin siRNA, or human antigen R (HuR) siRNA. The immunoreactivity of anti-β-actin antibody was analyzed at 72 h after transfection. **A**: Fibroblasts stained with Hoechst nuclear stain after treatment with scrambled siRNA. **B**: Immunoreactivity of fibroblasts with anti-β-actin antibody after treatment with scrambled siRNA. **C**: Fibroblasts stained with rhodamine-labeled phalloidin stain after treatment with scrambled siRNA. **D**: Overlay of (**A**), (**B**), and (**C**). **E**: Fibroblasts stained with Hoechst nuclear stain after treatment with GAPDH siRNA. **F**: Immunoreactivity of fibroblasts with anti-β-actin antibody after treatment with GAPDH siRNA. **G**: Fibroblasts stained with rhodamine-labeled phalloidin stain after treatment with GAPDH siRNA. **H**: Overlay of (**E**), (**F**), and (**G**). **I**: Fibroblasts stained with Hoechst nuclear stain after treatment with HuR siRNA. **J**: Immunoreactivity of fibroblasts with anti-β-actin antibody after treatment with HuR siRNA. **K**: Fibroblasts stained with rhodamine-labeled phalloidin stain after treatment with HuR siRNA. **L**: Overlay of (**I**), (**J**), and (**K**). **M**: Fibroblasts stained with Hoechst nuclear stain after treatment with β-actin siRNA. **N**: Immunoreactivity of fibroblasts with anti-β-actin antibody after treatment with β-actin siRNA. **O**: Fibroblasts stained with rhodamine-labeled phalloidin stain after treatment with β-actin siRNA, and (**P**): Overlay of (**M**), (**N**), and (**O**). Note that *β-actin* and *HuR* gene silencing affected β-actin expression. Scrambled siRNA transfection of normal corneal fibroblasts showed no effect on β-actin expression, whereas GAPDH siRNA treatment had a drastic effect on β-actin expression.

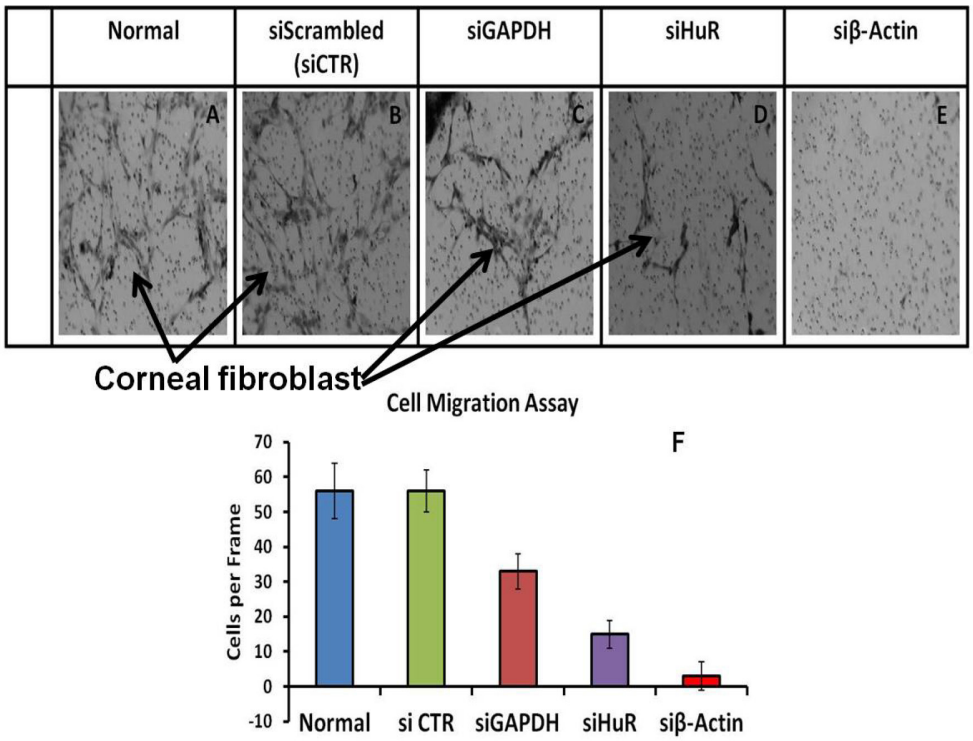

Figure 4. Analysis of cell migration after gene silencing (n = 4), using a modified Boyden chamber. Cell migration is shown with arrows. **A**: Migration of normal corneal fibroblast. **B**: Migration of cells after treatment with scrambled siRNA. **C**: Migration of cells after treatment of corneal fibroblast with GAPDH siRNA. **D**: Migration of cells after treatment of normal corneal fibroblast with human antigen R (HuR) siRNA. **E**: Migration of cells after treatment of normal corneal fibroblast with β-actin siRNA. **F**: Bar graph showing cell migration after different treatments (**A** to **E**). Cells were counted from six different frames. All the treatments were performed in tetraplicate, and standard deviations were calculated.

4F) were counted using Image-J software, incorporating multiple images and standard deviation analysis. Together, the results show that scrambled siRNA treatment had no effect on cell migration, which was identical to that of normal cell migration (Figure 4A,B). *GAPDH* gene silencing resulted in reduced cell migration compared to the scrambled siRNA. Silencing the *HuR* gene significantly decreased cell migration, whereas *β-actin* gene silencing abolished the migration. Although it is known that β-actin is an essential component of cell migration [15], the role of HuR in cell migration is shown for the first time in this report.

Effects of gene silencing on wound healing: Next we analyzed whether *HuR* gene silencing affects the migration and proliferation of corneal fibroblasts. A normal corneal fibroblast cell layer, grown to 85% confluency, was transfected with scrambled siRNA and siRNA of GAPDH, β-actin, or HuR, and the non-transfected cells were used as a control. A scratch wound was created at 72 h after transfection, and the dotted line in Figure 5 shows the wounded area. The images were taken at 0 h and 24 h post-scratch using a phase contrast microscope with a Nikon camera (Figure 5). The cells that migrated to the region between the dotted lines (wound) were counted from multiple images and the standard deviation determined (Figure 5K). Figure 5A,B shows the extent of the migration of the corneal fibroblasts at 0 h and 24 h post-scratch, respectively. Figure 5C–J shows the cell migration at 0 h and 24 h post-scratch following treatment with scrambled siRNA, GAPDH siRNA, HuR siRNA, or β-actin siRNA, respectively. The untreated normal corneal fibroblast layer had almost 100% wound closure in the region between the dotted lines (Figure 5B) with similar results observed with scrambled siRNA (Figure 5D). GAPDH siRNA treatment showed cell migration decreased after 24 h (Figure 5F), but greater decreased migration was seen in the cells treated with HuR siRNA (Figure 5H) or with β-actin siRNA (Figure 5J). Together, the results showed that the wound healing process was decreased after *GAPDH* gene silencing but a relatively greater decrease occurred with *HuR* and *β-actin* gene silencing. Figure 5K summarizes cell migration at 24 h after wound healing subjected to different siRNA treatments. Similarly, GAPDH siRNA treatment also resulted in decreased cell migration, GAPDH, an enzyme in the glycolytic pathway shown to have multiple functions, including an effect on cell motility during wound healing [16].

PI3K, is a known regulator of various cellular processes, including cell adhesion, vesicular trafficking, protein synthesis, cell growth, differentiation, cell survival, and cell transformation [17]. We performed a wound healing assay with Ly292004, a PI3K inhibitor, to examine how the inhibition of PI3K affects fibroblasts migration (Figure 6). Figure 6A,B,D,E,G,H shows cell migration at 0 h and 24 h post-scratch following treatment with scrambled siRNA, β-actin

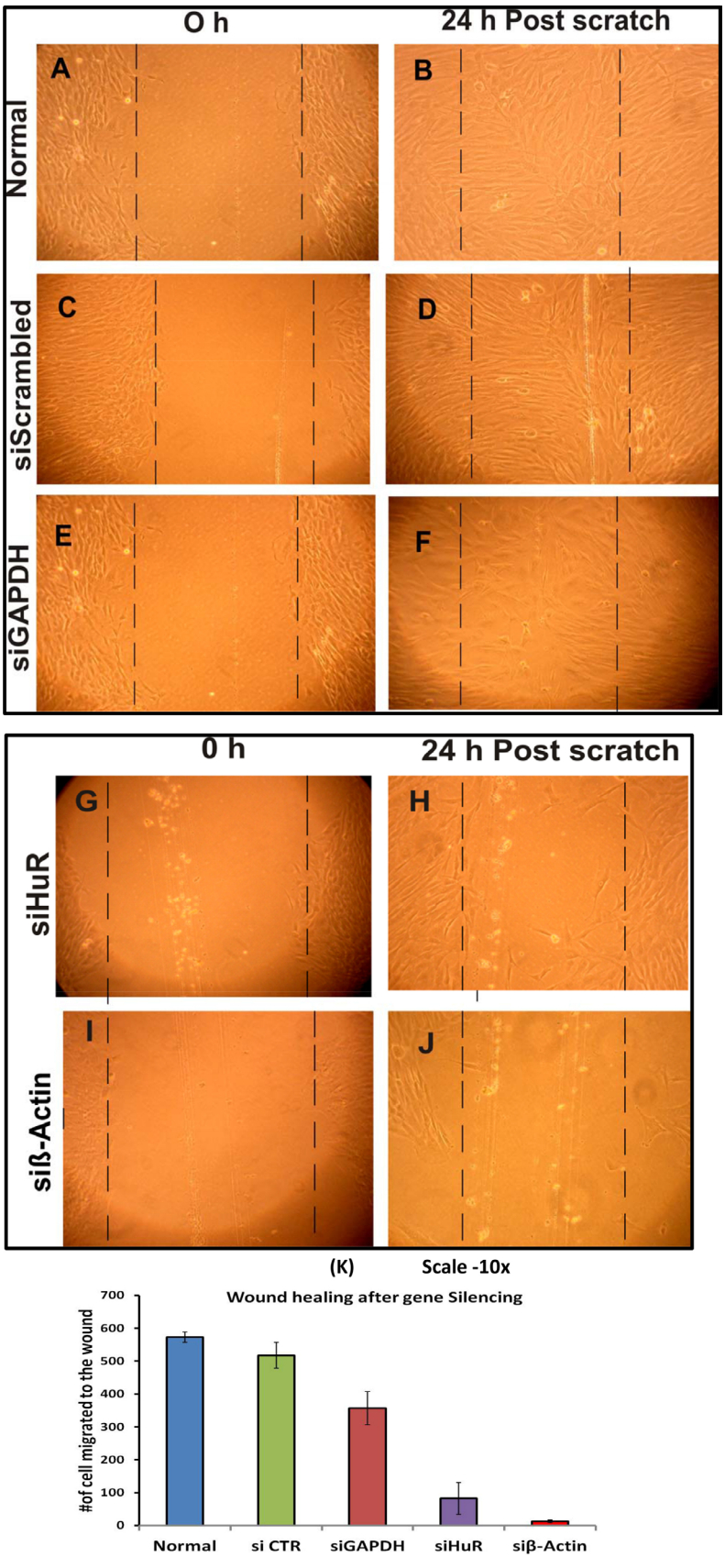

Figure 5. Effect of wound healing after gene silencing (n = 4). A scratch wound was created using 1 ml sterile serological pipette in a confluent corneal fibroblast culture after gene silencing of GAPDH, β-actin, or human antigen R (HuR). The images were taken at 0 h and 24 h. The dotted lines show the area where the scratch wound was created. **A**: Normal cells with a scratch wound at 0 h. **B**: Cells migrating to the site of wound after 24 h. **C**: Scratch wound at 0 h in cells that were treated with scrambled siRNA. **D**: Migration of cells to the site of wound after 24 h in cell culture that was treated with scrambled siRNA. **E**: Scratch wound at 0 h in cells that were treated with GAPDH siRNA. **F**: Migration of cells to the site of wound after 24 h that were treated with scrambled siRNA. **G**: Scratch wound at 0 h in cells that were treated with HuR siRNA. **H**: Migration of cells to the site of wound after 24 h that were treated with HuR siRNA. **I**: Scratch wound at 0 h in cells that were treated with β-actin siRNA. **J**: Cells migrated to the site of wound after 24 h in cells that were treated with β-actin siRNA. **K**: A bar graph showing the number of cells that migrated after 24 h following the scratch wound in cells treated with siScrambled, siGAPDH, siHuR, or siβ-actin. The scratch wound assay was performed in tetraplicate, and standard deviations were calculated.

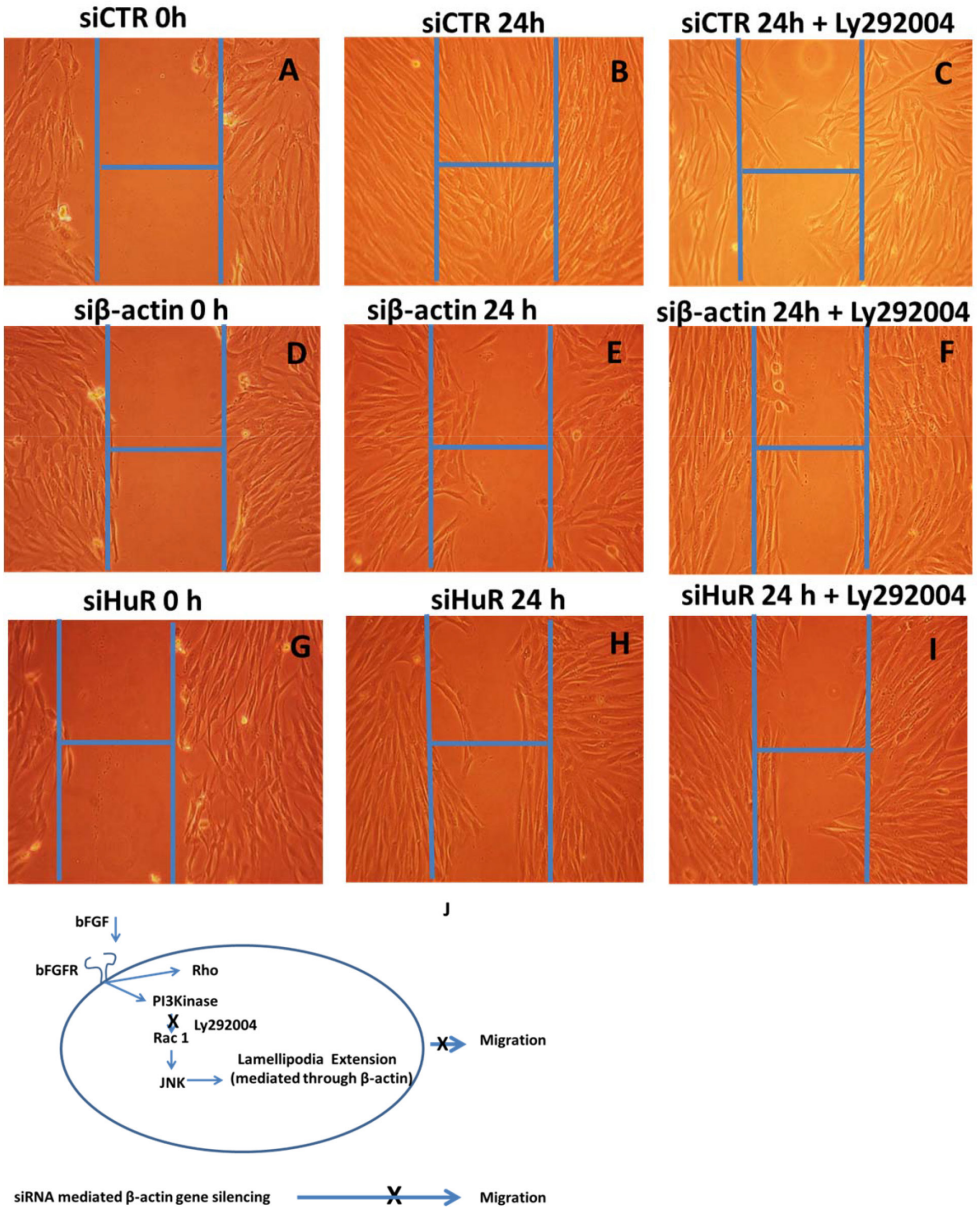

Figure 6. Effect of phosphatidylinositol 3-kinase inhibitor on wound healing after gene silencing (n = 4). The scratch wound was created using 1 ml sterile serological pipette in a confluent corneal fibroblast culture after gene silencing of β-actin or human antigen R (HuR). The images were taken at 0 h and 24 h. The lines show the area where the scratch wound was created. **A**: Scratch wound at 0 h in cells that were treated with scrambled siRNA. **B**: Migration of cells to the site of the wound after 24 h in cells that was treated with scrambled siRNA. **C**: Migration of cells to the site of the wound after 24 h in cells that were treated with scrambled siRNA + phosphatidylinositol 3-kinase (PI3K) inhibitor Ly292004. **D**: A scratch wound at 0 h in cells that were treated with β-actin siRNA. **E**: Migration of cells to the site of the wound after 24 h that were treated with β-actin siRNA. **F**: Migration of cells to the site of wound after 24 h in cells that was treated with β-actin siRNA +PI3 kinase inhibitor Ly292004. **G**: A scratch wound at 0 h in cells that were treated with HuR siRNA. **H**: Migration of cells to the site of the wound after 24 h in cells that were treated with HuR siRNA. **I**: Migration of cells to the site of the wound after 24 h in cells that was treated with HuR siRNA +PI3 kinase inhibitor Ly292004. The scratch wound assay was performed in tetraplicate. **J**: A schematic representation of PI3K-induced actin filament remodeling and migration.

siRNA, or HuR siRNA, respectively. Similarly, Figure 6C,F,I shows the results of PI3K inhibition using LY292004 after 24 h. After 24 h post-scratch, the untreated cells migrated to the wound (Figure 6B) where on PI3K inhibition, severely impaired wound healing occurred (Figure 6C). *β-Actin* and *HuR* gene silencing resulted in inhibition of wound healing after 24 h post-scratch as seen in Figure 6E,H, respectively. The inhibition of PI3K and gene silencing had the same effects as that of gene silencing alone (Figure 6F,I). Figure 6J shows the downstream pathway of PI3K, and its inhibition would have a similar effect as that of *β-actin* and *HuR* gene silencing.

DISCUSSION

Our previous report showed that the expression levels of β-actin and HuR were downregulated in the human keratoconic corneal stroma but not in the normal corneal stroma [12]. In the present study, we used gene silencing to determine the functional properties of β-actin, and whether *HuR* gene silencing affects *β-actin* gene expression in cultured

fibroblasts derived from the keratocytes of normal human corneas. Gene silencing using RNA interference has been a popular method for in vitro gene functional studies using a method in which introducing dsRNA, homologous in sequence to the silenced gene, results in post-transcriptional gene silencing [18].

Our RT–PCR analysis showed that gene silencing of *β-actin* or *HuR* for 24 h resulted in downregulation of *β-actin* gene expression. The silencing of the *HuR* gene also resulted in downregulation of *β-actin* gene expression. The levels of *β-actin* and *HuR* gene expression were reduced by 72% and 64% after *β-actin* and *HuR* gene silencing, respectively. The mRNA of HuR is ubiquitously expressed in all proliferating cells, and it is the most important post-transcriptional regulator of gene expression [9]. HuR binding to the U-rich element is involved in mRNA stability [5,11], and prolongs the half-life of β-actin mRNA [10]. Together, our present study showed that silencing the *HuR* gene resulted in downregulation of β-actin at the transcriptional and translational levels in corneal fibroblasts. This downregulation could be due to the loss of HuR, a stability factor for β-actin mRNA. These expression levels were downregulated for up to 96 h post-siRNA treatment (results not shown).

In the present study, the immunohistochemical-confocal imaging technique was used to localize proteins that were affected by gene silencing. When the *HuR* gene was silenced, its expression was decreased, but its expression was not affected after the *GAPDH* gene, the *β-actin* gene, or scrambled siRNA (data not shown) was silenced. Gene silencing of either the *HuR*- or *β-actin* gene resulted in decreased expression of the *β-actin* gene. Therefore, the *HuR* gene has a regulatory role in β-actin expression, which was confirmed at translational levels with confocal imaging. Surprisingly, *β-actin* gene expression was also decreased after the *GAPDH* gene was silenced (Figure 3F). This could be due to diverse functions of GAPDH, such as DNA repair [19], tRNA export [20], and in cell death [21,22]. GAPDH is also known to interact with tubulin and actin and thus plays a role in cytoskeleton dynamics [23].

Actin isoforms have highly conserved amino acid sequences. Gama-actin expression was not affected when the *β-actin* gene was silenced in normal corneal fibroblasts (data not shown). Cell culture studies have shown that β- and γ-actins have distinct physiologic roles. In the motile cells, β-actin accumulates at the leading edge, and γ-actin tends to be at the stress fibers [24]. Complementing this was the finding that the β-actin mRNA was located at the leading edge of the moving fibroblast whereas γ-actin was localized at the stress fibers [25]. Recent studies using knockout mouse models have also shown that β-actin and γ-actins show distinct phenotypes. This is further supported by the fact that in a β-actin knockout mouse, the embryonic fibroblasts showed a decreased G-actin pool compared to F-actin [15]. Our results also showed positive F-actin staining in fibroblasts that showed the absence of β-actin staining in normal fibroblasts following *β-actin* gene silencing. The presence of F-actin staining could be due to the presence of γ-actin in these cells. This could also be due to the absence of the monomeric G-actin pool, which could lead to increased expression of megakaryoblastic leukemia (MAL also known as MKL) gene ID 89880, OMIM 60607; serum response factor (SRF) gene ID 6722 , OMIM 600589 (*MAL-SRF*) target genes. Monomeric actins are known to inhibit coactivator MAL-SRF [26] and α-smooth muscle actin.

One of the major functions of β-actin, but not that of γ-actin, is in cell motility [27]. Overexpression of the *β-actin* gene results in plasma membrane protrusions and cell migration [28]. Our cell motility analysis using Boyden chambers showed that gene silencing of β-actin drastically reduced the cell migration (Figure 4E). Cell migration was also decreased when HuR was downregulated (Figure 4D) but was unaffected in untreated cells or those treated with scrambled siRNA. Cell motility is an important feature of multicellular organisms, maintained by actin-based protrusions such as lamellipodia, ruffles, and filopodia [29]. We observed for the first time that *GAPDH* gene silencing also affected cell migration, possibly by way of its known function as an actin-binding protein. It has been recently reported that glycolytic enzymes, which included GAPDH, are associated with actin and other membrane proteins [30]. This association might satisfy the high ATP energy demand during actin dynamics.

Keratocytes repopulate the stroma at the site of an injury by a combination of proliferation and migration, which is stimulated by cytokines released from the epithelium [31]. This leads to a series of events that causes the keratocyte transformation to fibroblasts and myofibroblasts, and irregular spacing of collagen fibrils [32]. Silencing of the *β-actin* and *HuR* genes resulted in a significant decrease in wound healing as evidenced by the decrease in the cell migration in a scratch-wound gap in a confluent cell layer (Figure 5H,J). In contrast, complete wound healing occurred in normal corneal fibroblasts, and those treated with scrambled siRNA, whereas GAPDH siRNA also showed decreased cell migration. Together, the results suggest the importance of β-actin and HuR in cell motility during wound healing. The unexpected role of GAPDH in cell migration and proliferation requires further study.

The actin cytoskeleton is indispensable for wound repair, and PI3K is one of the key enzymes involved in this process [33]. Small G-protein, Rac1, which is an effector of PI3K, mediates stress-activated kinase c-Jun N-terminal kinases (JNKs), and is essential for basic fibroblastic growth factor (bFGF)-induced fibroblast migration [33]. A specific inhibitor of PI3K, LY292004, causes significant inhibition of cell growth and migration. Our results also show inhibition of PI3K by LY292004 significantly inhibited cell growth and migration in siCTR cells (Figure 6J). This was similar to cells that had undergone *β-actin* or *HuR* gene silencing. The absence of β-actin monomers (an effect of *β-actin* gene knockdown) hinders actin cytoskeleton polymerization and thus affects cell migration and proliferation. This result was similar to that of inhibition of PI3K (Figure 6J) and an upstream element in the pathway (Figure 6J).

In summary, our findings show that downregulation of the *HuR* gene significantly reduces *β-actin* gene expression, and affects the migration and proliferation of corneal fibroblasts. These results also confirm our earlier findings that downregulation of the *β-actin* gene in keratoconus corneal stromal keratocytes is due to downregulation of the *HuR* gene. Our future work will explore the significance of downregulation of the *β-actin* and *HuR* genes in the progression of keratoconus disease.

ACKNOWLEDGMENTS

The authors thank the Alabama Eye Bank for providing normal corneas for the study. The study was partly supported by a NIH grant NEI P30EYE3039.

REFERENCES

1. Bassell G, Singer RH. mRNA and cytoskeletal filaments. Curr Opin Cell Biol 1997; 9:109-15. [PMID: 9013679].
2. Herman IM. Actin Isoforms. Curr Opin Cell Biol 1993; 5:48-55. [PMID: 8448030].
3. Harborth J, Elbashir SM, Bechert K, Tuschl T, Weber K. Identification of essential genes in cultured mammalian cells using small interfering RNAs. J Cell Sci 2001; 114:4557-65. [PMID: 11792820].
4. Shawlot W, Deng JM, Fohn LE, Behringer RR. Restricted β-galactosidase expression of a hygromycin-lacZ gene targeted to the β- actin locus and embryonic lethality of β-actin mutant mice. Transgenic Res 1998; 7:95-103. [PMID: 9608737].
5. Olave IA, Reck-Peterson SL, Crabtree GR. Nuclear actin and actin-related proteins in chromatin remodeling. Annu Rev Biochem 2002; 71:755-81. [PMID: 12045110].
6. Kislauskis EH, Li Z, Singer RH, Taneja KL. Isoform-specific 3′-untranslated sequences sort alpha-cardiac and beta-cytoplasmic actin messenger RNAs to different cytoplasmic compartments. J Cell Biol 1993; 123:165-72. [PMID: 8408195].
7. Abe R, Sakashita E, Yamamoto K, Sakamoto H. Two Different RNA Binding Activities for the AU-Rich Element and the Poly(A) Sequence of the Mouse Neuronal Protein mHuC. Nucleic Acids Res 1996; 24:4895-901. [PMID: 9016658].
8. Ma W-J, Chung S, Furneaux H. The Elav-like proteins bind to AU-rich elements and to the poly(A) tail of mRNA. Nucleic Acids Res 1997; 25:3564-9. [PMID: 9278474].
9. Fan XC, Steitz JA. Overexpression of HuR, a nuclear-cytoplasmic shuttling protein, increases the in vivo stability of ARE-containing mRNAs. EMBO J 1998; 17:3448-60. [PMID: 9628880].
10. Dormoy-Raclet V, Ménard I, Clair E, Kurban G, Mazroui R, Di Marco S, von Roretz C, Pause A, Gallouzi IE. The RNA-binding protein HuR promotes cell migration and cell invasion by stabilizing the beta-actin mRNA in a U-rich-element-dependent manner. Mol Cell Biol 2007; 27:5365-80. [PMID: 17548472].
11. Condeelis J, Singer RH. How and why does beta-actin mRNA target? Biol Cell 2005; 97:97-110. [PMID: 15601261].
12. Joseph R, Srivastava OP, Pfister RR. Downregulation of β-Actin Gene and Human Antigen R in Human Keratoconus. Invest Ophthalmol Vis Sci 2012; 53:4032-41. [PMID: 22562506].
13. UK L. Cleavage of structural proteins during the assembly of the head of bacteriophage T4. Nature 1970; 227:680-5. [PMID: 5432063].
14. Schneider CARW, Eliceiri KW. NIH Image to ImageJ: 25 years of image analysis. Nat Methods 2012; 9:671-5. [PMID: 22930834].
15. Bunnell TM, Burbach BJ, Shimizu Y, Ervasti JM. β-Actin specifically controls cell growth, migration and the G-actin pool. Mol Biol Cell 2011; 22:4047-58[PMID: 21900491].
16. Knull HRWJ. Association of glycolytic enzymes with the cytoskeleton. Curr Top Cell Regul 1992; 33:15-30. [PMID: 1499331].
17. . Krasilnikov MA. Phosphatidylinositol-3 kinase dependent pathways: the role in control of cell growth, survival, and malignant transformation. Biochemistry (Mosc) 2000; 65:59-67. [PMID: 10702641].
18. Elbashir SM, Harborth J, Weber K, Tuschl T. Analysis of gene function in somatic mammalian cells using small interfering RNAs. Methods 2002; 26:199-213. [PMID: 12054897].
19. Meyer-Siegler K, Mauro DJ, Seal G, Wurzer J, deRiel JK, Sirover MA. A human nuclear uracil DNA glycosylase is the 37-kDa subunit of glyceraldehyde-3-phosphate dehydrogenase. Proc Natl Acad Sci USA 1991; 88:8460-4. [PMID: 1924305].

20. Singh R, Green M. Sequence-specific binding of transfer RNA by glyceraldehyde-3-phosphate dehydrogenase. Science 1993; 259:365-8. [PMID: 8420004].

21. Hara MR, Agrawal N, Kim SF, Cascio MB, Fujimuro M, Ozeki Y, Takahashi M, Cheah JH, Tankou SK, Hester LD, Ferris CD, Hayward SD, Snyder SH, Sawa A. S-nitrosylated GAPDH initiates apoptotic cell death by nuclear translocation following Siah1 binding. Nat Cell Biol 2005; 7:665-74. [PMID: 15951807].

22. Sawa A, Khan AA, Hester LD, Snyder SH. Glyceraldehyde-3-phosphate dehydrogenase: Nuclear translocation participates in neuronal and nonneuronal cell death. Proc Natl Acad Sci USA 1997; 94:11669-74. [PMID: 9326668].

23. Kumagai H, Sakai H. A Porcine Brain Protein (35K Protein) which Bundles Microtubules and Its Identification as Glyceraldehyde 3-Phosphate Dehydrogenase. J Biochem 1983; 93:1259-69. [PMID: 6885722].

24. Hoock TC, Newcomb PM, Herman IM. Beta actin and its mRNA are localized at the plasma membrane and the regions of moving cytoplasm during the cellular response to injury. J Cell Biol 1991; 112:653-64. [PMID: 1993736].

25. Lawrence JB, Singer RH. Intracellular localization of messenger RNAs for cytoskeletal proteins. Cell 1986; 45:407-15. [PMID: 3698103].

26. Vartiainen MK, Guettler S, Larijani B, Treisman R. Nuclear Actin Regulates Dynamic Subcellular Localization and Activity of the SRF Cofactor MAL. Science 2007; 316:1749-52. [PMID: 17588931].

27. Bunnell TM, Ervasti JM. Delayed embryonic development and impaired cell growth and survival in Actg1 null mice. Cytoskeleton. 2010; 67:564-72. [PMID: 20662086].

28. Peckham M, Miller G, Wells C, Zicha D, Dunn GA. Specific changes to the mechanism of cell locomotion induced by overexpression of (β)-actin. J Cell Sci 2001; 114:1367-77. [PMID: 11257002].

29. Small JV, Stradal T, Vignal E, Rottner K. The lamellipodium: where motility begins. Trends Cell Biol 2002; 12:112-20. [PMID: 11859023].

30. Puchulu-Campanella E, Chu H, Anstee DJ, Galan JA, Tao WA, Low PS. Identification of the Components of a Glycolytic Enzyme Metabolon on the Human Red Blood Cell Membrane. J Biol Chem 2013; 288:848-58[PMID: 23150667].

31. Wilson SE, Mohan RR, Mohan RR, Ambrósio R Jr, Hong J, Lee J. The Corneal Wound Healing Response: Cytokine-mediated Interaction of the Epithelium, Stroma, and Inflammatory Cells. Prog Retin Eye Res 2001; 20:625-37. [PMID: 11470453].

32. Hassell JR, Kublin C, Newsome DA. Proteoglycan changes during restoration of transparency in corneal scars. Arch Biochem Biophys 1983; 222:362-9. [PMID: 6847191].

33. Kanazawa S, Fujiwara T, Matsuzaki S, Shingaki K, Taniguchi M, Miyata S, Tohyama M, Sakai Y, Yano K, Hosokawa K, Kubo T. bFGF regulates PI3-kinase-Rac1-JNK pathway and promotes fibroblast migration in wound healing. PLoS ONE 2010; 5:e12228-[PMID: 20808927].

Articles are provided courtesy of Emory University and the Zhongshan Ophthalmic Center, Sun Yat-sen University, P.R. China. The print version of this article was created on 2 May 2014. This reflects all typographical corrections and errata to the article through that date. Details of any changes may be found in the online version of the article.